Application of LPV Modeling, Design and Analysis Methods to a Re-entry Vehicle

Andrés Marcos*,
Deimos Space S.L.U., Madrid, 28760, Spain

Joost Veenman†, Carsten Scherer†,
Department of Mathematics, University of Stuttgart, Pfaffenwaldring 57, 70569 Stuttgart, Germany

Gabriele De Zaiacomo‡, David Mostaza‡, Murray Kerr‡
Deimos Space S.L.U., Madrid, 28760, Spain

Hakan Köroğlu†
Dept. Elect. Eng., Technische Universiteit Eindhoven, Postbus 513, 5600 MB Eindhoven, The Netherlands

Samir Bennani§
ESA ESTEC, Noordwijk, 2200, The Netherlands

In this paper the application of linear parameter varying (LPV) modeling, design and analysis methods to a re-entry vehicle is presented. The selected atmospheric re-entry benchmark includes full nonlinear motion, a detailed aerodynamic database (from hypersonic to subsonic), relevant actuator and sensor models and physically-meaningful aerodynamic and parametric uncertainty profiles. The results show that: (i) LPV controller design methods can solve gain-scheduling problems in a very effective manner, (ii) integral quadratic constraint (IQC) analysis methods can be used very efficiently to accurately interpret the nonlinear time domain simulation results, and, (iii) the use of linear fractional transformation (LFT) and LPV modeling representations are key to a successful analysis.

I. Introduction

During the last 30 years there has been an increasing interest in linear parameter varying (LPV) techniques for space applications due to their potential to handle practical issues such as controller scheduling, time-varying parameters and reduced mode complexity within a coherent design framework [24]. However, since the control design process followed in space application is very cautious, it is crucial to showcase in a transparent manner their practical advantages in order to ensure a successful industrial transfer of the LPV techniques. Additionally, the development of reliable software tools has been identified as a key factor in the slow introduction of LPV techniques in space industry.

This paper presents a summary of the final results of a European Space Agency (ESA) funded study with the task of developing such LPV tools and showcasing their effectiveness. The study is entitled "LPV modeling, analysis and design (LPVMAD)". Recently, the results of Phase I of the project were presented, using simplified atmospheric re-entry study cases [15, 16, 17, 18, 19, 24]. This paper, on the other hand, focuses on the results of Phase II in which an enhanced version of the NASA HL-20 atmospheric re-entry vehicle is considered [25, 26, 27, 28]. The goal of the second phase of the LPVMAD study is to demonstrate the effectiveness of LPV techniques to deal with some of the practical issues found in space control design projects. An example of these issues are controller scheduling, time-varying behavior and analytical mismatch between the linear and nonlinear results –all

* LPVMAD project manager. Email: andres.marcos@deimos-space.com. AIAA senior member.
†Formerly with Delft University of Technology, Delft, The Netherlands. Email: <jveenman>,<carsten.scherer >@mathematik.uni-stuttgart.de
‡ Deimos Space S.L.U. Email: <gabriele.dezaiacomo>,<david.mostaza>,<murray.kerr>@deimos-space.com.
§ LPVMAD technical officer, ESA ESTEC. Email: samir.bennani@esa.int

of which typically increase the time and cost required to obtain a validated controller. The results show that for the selected challenging space applications:

- LPV design techniques, in comparison to the more traditional gain-scheduled techniques, are capable of generating automatically scheduled controllers that fulfill the design requirements in a much more systematic and efficient manner.
- LPV/LFT modeling techniques are the key ingredient to apply advanced LPV analysis and synthesis techniques and allow us to include critical time-varying and/or uncertain system behavior.
- LPV analysis techniques, such as integral quadratic constraint (IQC) methods, can handle, in a reliable and transparent fashion, nonlinear and time-varying behavior, resulting in an effective bridge between the widespread but limited analytical linear analysis and the costly nonlinear Monte Carlo analysis campaigns.

The paper is organized as follows. Section II provides an overview of the LPVMAD study as well as of the re-entry benchmark. Section III presents the baseline gain-scheduling H_∞ [31] and advanced LPV controller designs, including a comparative summary of the Monte Carlo nonlinear simulation campaigns. Section IV and Section V detail respectively the development of the LPV/LFT models and the results of the IQC analysis obtained with these models. Finally, Section VI presents the conclusions.

II. LPVMAD study and the re-entry benchmark problem

The European Space Agency addressed an envisioned need for advanced gain scheduling techniques in space applications by establishing an industrial-academia consortium with the task of developing an industrial LPV control design framework supported by reliable LPV software tools. The "LPV Modeling, Analysis and Design (LPVMAD)" consortium, led by Deimos Space (Spain) and composed by research teams from the Computer and Automation Research Institute (SZTAKI, Hungary), Delft University of Technology (The Netherlands) and Leicester University (United Kingdom), was formed to address this need. The project objectives were:

- To assess the applicability and needs of LPV techniques in the control design process for space applications
- To propose an LPV control design framework
- To develop reliable LPV/LFT modeling, analysis and design tools to support such a framework
- To demonstrate the effectiveness of the developed framework and tools for a relevant space application

The results of Phase I of the project revealed a successful accomplishment of the first three project objectives [15, 16, 17, 18, 19, 24]. During this first phase, two simplified study cases were used to validate the developed tools and to expose the benefits and characteristics of the selected LPV techniques in a transparent and incremental fashion. In the second phase of the LPVMAD project, the fourth and last objective is addressed. The selected benchmark problem is the well-known NASA HL-20 atmospheric re-entry vehicle, and includes practical issues such as saturation, motion coupling, controller scheduling and time-varying behavior.

A. The enhanced NASA HL-20 atmospheric re-entry vehicle

The HL-20 lifting-body vehicle, shown in Figure II-1, was proposed as a substitute to the Space Shuttle Orbiter. Although it was finally de-commissioned much research effort was devoted to developing a fairly detailed aerodynamic database for the complete speed range of the vehicle [25, 26, 27, 28].

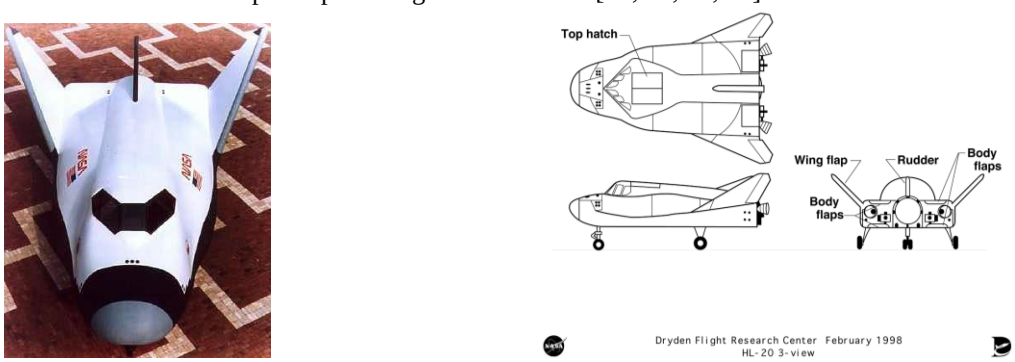

Figure II-1 NASA HL-20 test platform and 3-view [Courtesy of NASA Dryden FRC]

An optimized 3 degrees of freedom guidance trajectory adapted from reference [30] is considered. The trajectory covers the HL-20 re-entry from the Entry Interface (EI) down to the Heading Alignment Circle (HAC) acquisition, i.e. from Mach 20 to 1.5 and an altitude of 122Km down to 17 Km. Although the trajectory can be divided into four sub-phases, the present study focuses on the full aerodynamic phase corresponding to the terminal energy approach management (TAEM), approximately from low supersonic to sub-sonic speeds, i.e. Mach$\in$[3,0.8]. As shown in Figure II-2, the selected phase represents the end of a bank reversal and a similar maneuver for the angle-of-attack.

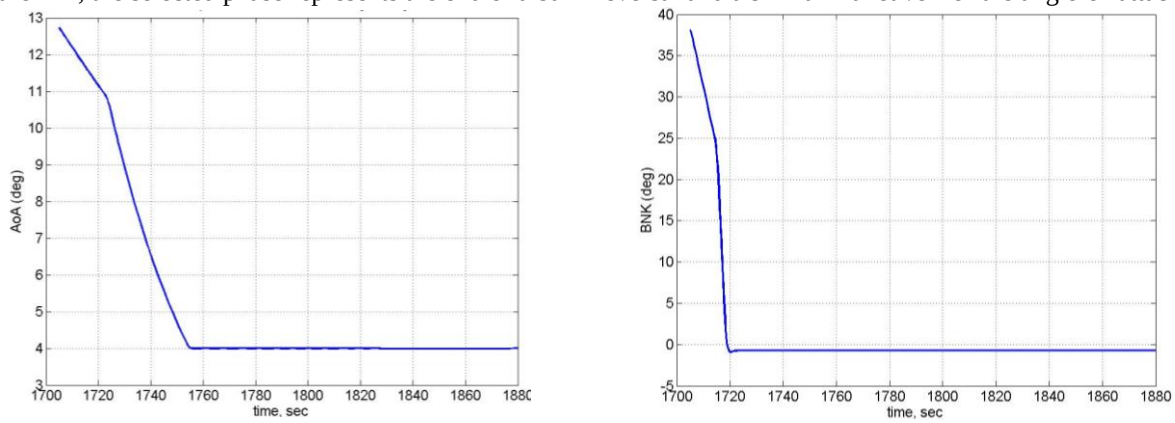

Figure II-2 Nominal reference trajectories for the angle-of-attack and the bank angle with respect to time

The full nonlinear equations of motion [25] are considered together with a representative aerodynamic database, taken from NASA reports [25, 26, 27, 28]. The implementation of the HL-20 model is much more advanced and representative than the publicly available model provided in [29], which uses the polynomial simplifications given in [26]. The complete aerodynamic database is formed by nonlinear look-up tables (LUT) that depend on Mach number, angle-of-attack, sideslip and control surface deflections. These LUTs represent the specific stability derivatives, which are subsequently added to obtain the aerodynamic coefficients–see [25] for an explanation of the stability derivatives:

CL = CL0 + CLBFUL + CLBFUR + CLBFLL + CLBFLR + CLWFL + CLWFR + CLRUD (1)

CD = CD0 + CDBFUL + CDBFUR + CDBFLL + CDBFLR + CDWFL + CDWFR + CDRUD (2)

CM = CM0 + CMBFUL + CMBFUR + CMBFLL + CMBFLR + CMWFL + CMWFR + CMRUD + CMQ*QCO2V (3)

CY = CYBFUL + CYBFUR + CYBFLL + CYBFLR +CYWFL + CYWFR + CYRUD + CYB*BETA (4)

CN = CNBFUL + CNBFUR + CNBFLL + CNBFLR +CNWFL + CNWFR + CNRUD + CNB*BETA +CNP*PBO2V + CNR*RBO2V (5)

CR = CRBFUL + CRBFUR + CRBFLL + CRBFLR + CRWFL + CRWFR + CRRUD + CRB*BETA +CLP*PBO2V + CLR*RBO2V (6)

The available control surfaces are the upper left- and right-flaps (DUL and DUR), the lower left- and right-flaps (DLL and DLR), the wing left- and right-flaps (DEL and DER) and the rudder (DR). The deflection is positive downward for the upper/lower flaps (+TED and -TEU), away from the vehicle for the wing flaps (+TED) and to the left for the rudder (+TEL). The nonlinear model implements a control surface mix logic based on controller-commanded elevator deflection δ_{ele}, aileron deflection δ_{ail}, te speed-brake deflection $\delta_{sbk,}$ rudder deflection δ_{rud} and Mach number:

$$\begin{aligned} DEL &= DER = \delta_{ele} \\ DUL &= DUR = f_1(\delta_{ele}, \delta_{ail}, \delta_{sbk}, M) \\ DLL &= DLR = f_2(\delta_{ele}, \delta_{ail}, \delta_{sbk}, M) \\ DR &= \delta_{rud} \end{aligned} \tag{7}$$

The output of the control-mixer is passed to the actuation system. Each actuation system is composed of a series interconnection of a second order filter, a magnitude limiter, a rate limiter and a time delay (of 0.005 seconds). The sensor system is implemented as a first order coloring filter with measurement-dependent crossover frequencies as well as a bias driven by Gaussian white noise (obtained by a band-limited white noise generator with a noise power of one and a sample time of 0.01 seconds).

The two key arguments for proposing this re-entry benchmark problem are its highly nonlinear nature and the high physical fidelity of the models. Moreover, some of the modeled parameters within the physical model are

assumed to be uncertain. Table II-3 shows the nominal values and percentage uncertainty ranges used in the HL-20 re-entry vehicle for the main vehicle geometry as well as the aerodynamic coefficients. Note that the $C_{L/D}$ uncertainty profile serves to physically relate the uncertainties from the lift (CL) and drag (CD) coefficients.

Table II-3 Uncertain parameters of HL-20 vehicle: nominal value and uncertainty range

	Nominal	**$\Delta_{\%}$ range (uniform distribution)**
X_{CG} [m]	$0.555L_{ref} = 4.7772$	± 0.5
I_{XX} [Kgm^2]	1.0185e+4	± 5
I_{YY} [Kgm^2]	4.5547e+4	± 5
I_{ZZ} [Kgm^2]	4.8327e+4	± 5
Mass [Kg]	8660	± 5
Y_{CG} [m]	0	± 0.002
Z_{CG} [m]	0	± 0.01
I_{Xz} [Kgm^2]	0	± 50
C_D, C_L, C_M, C_Y, C_l, C_n, $C_{L/D}$	Calculated on-line	Changes with Mach number

A multiplicative uncertainty model is considered around the nominal value u, based on the percentage uncertainty range $\Delta_{\%}$ shown in Table II-3 and the normalized random but bounded gain δ_U, i.e. $u_\Delta=(1+\ \delta_U\ \Delta_{\%})u$. For those magnitudes with nominal value equal to zero, an additive model is employed (the multiplicative model would not introduce uncertainty in the parameter for these cases). Finally, the aerodynamic database, as given in the NASA reports [25, 26, 27, 28], shows quite nonlinear behavior and alternates stable with unstable phases (notice the positive and negative slopes in C_{MO} shown in Figure II-4).

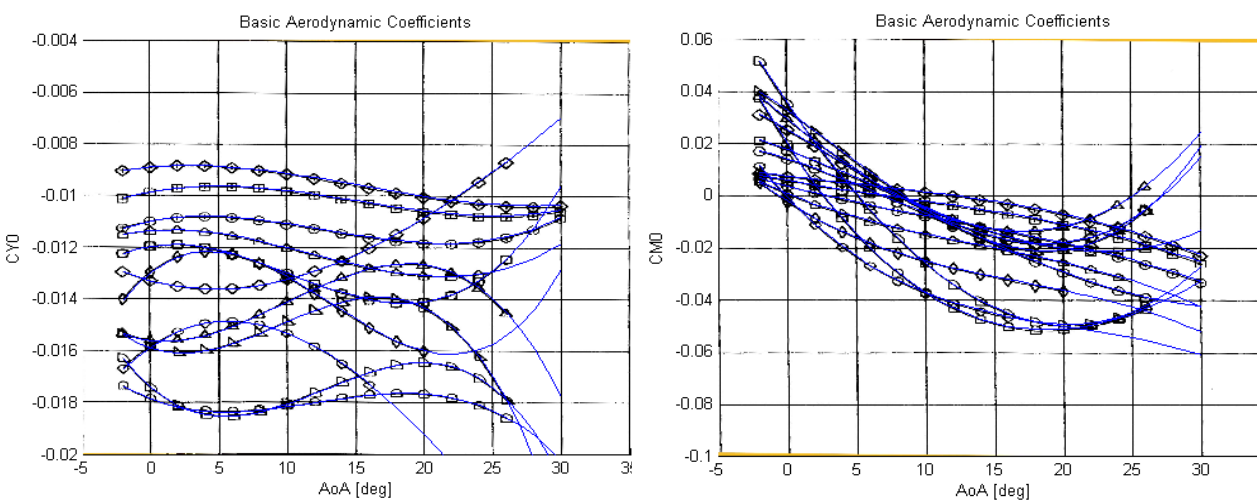

Figure II-4 Basic aerodynamic coefficients in terms of the angle-of-attack and Mach

B. Analysis of the enhanced NASA HL20 atmospheric re-entry vehicle

In this section, a linear analysis of the stability and frequency response characteristics of the open loop LTI plants for the longitudinal and lateral/directional motion is provided to showcase the representative challenges that the developed industrial benchmark entails.

Longitudinal motion

Figure II-5 shows the pole/zero maps for a number of LTI longitudinal plants for different Mach numbers along the full re-entry trajectory from Mach 20 down to 0.8. Notice the large variation of the damping and frequencies over the whole Mach interval, especially in the region below Mach 1.5 (in agreement with the C_{MO} characteristic from Figure II-4). Nevertheless, despite the stability change, the variations are typical in this type of vehicle and are sufficiently smooth to indicate a "relatively easy" design task for the decoupled longitudinal motion.

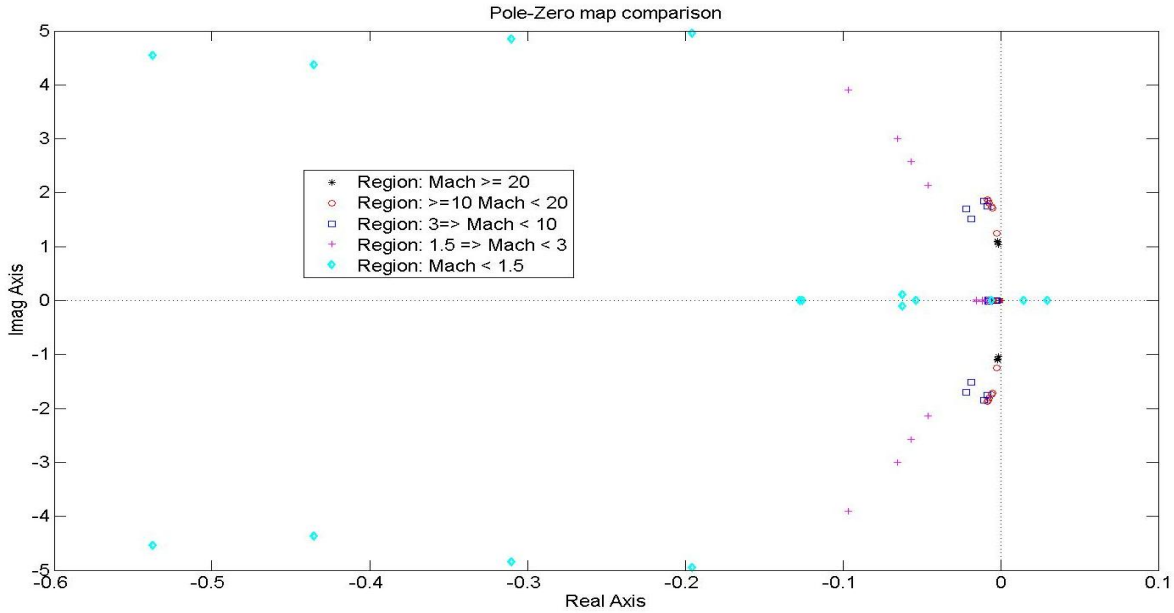

Figure II-5 Dynamic variations in the longitudinal motion: Pole/Zero map based on Mach regions

Looking at the Bode plots from Figure II-6, the phase responses show, again, the change in stability for M<1.5 while the magnitude plots show a variability in the natural frequency of the short-period mode of almost 10 radians/seconds (the peaks from the logarithmic frequency range from 10^0 to 10^1). Moreover, the plots show a change in the DC gain along the Mach trajectory that cannot be neglected.

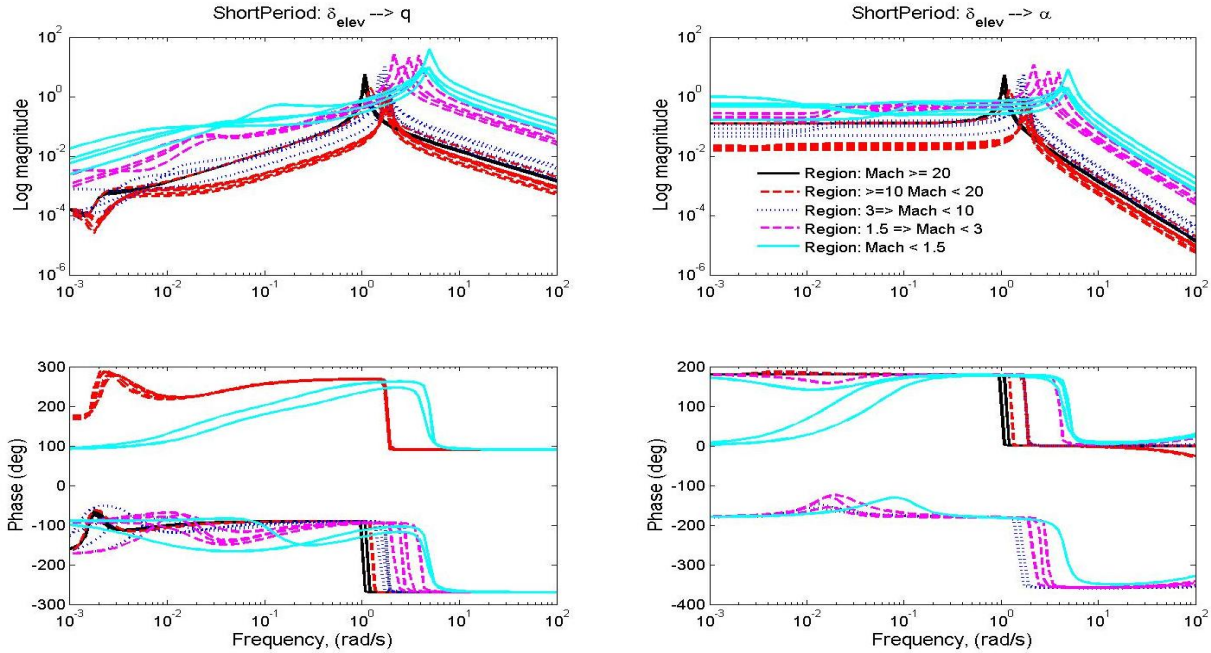

Figure II-6 Dynamic variations in the longitudinal motion: Bode plots based on Mach regions

Lateral/Directional motion

The corresponding analysis for the lateral/directional motion yields similar conclusions, however, to a larger and more critical extend. Figure II-7 shows the pole/zero map for the region of interest i.e. Mach∈[3.0, 0.8]. Based on Figure II-7 it can be concluded that the design of a controller that performs sufficiently well is a very challenging problem. Moreover, due to the number of changes between stability and instability, it is unlikely that it is possible to design a single LTI controller for the whole Mach interval.

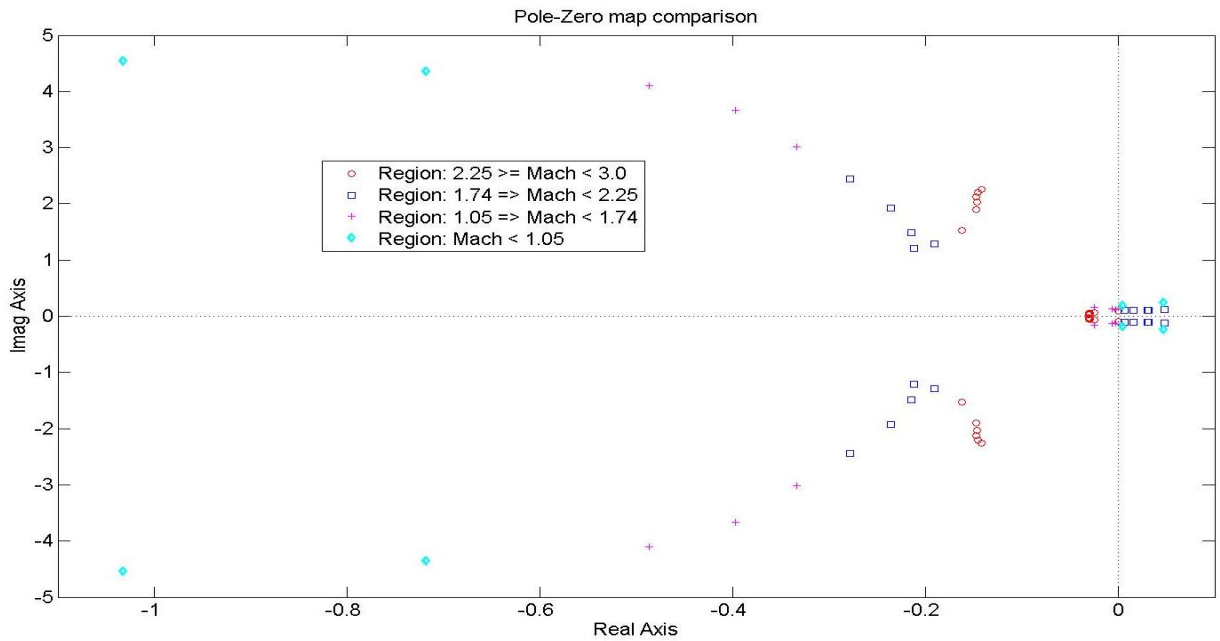

Figure II-7 Dynamic variations in the lateral/directional motion: Pole/Zero map based on Mach regions

Figure II-8 shows the Bode frequency responses of the transfer functions from the aileron deflection to the lateral/directional states. As can be seen, there are, if compared to the longitudinal motion, slightly less DC variations. However, there are similar peak ranges over the whole Mach interval.

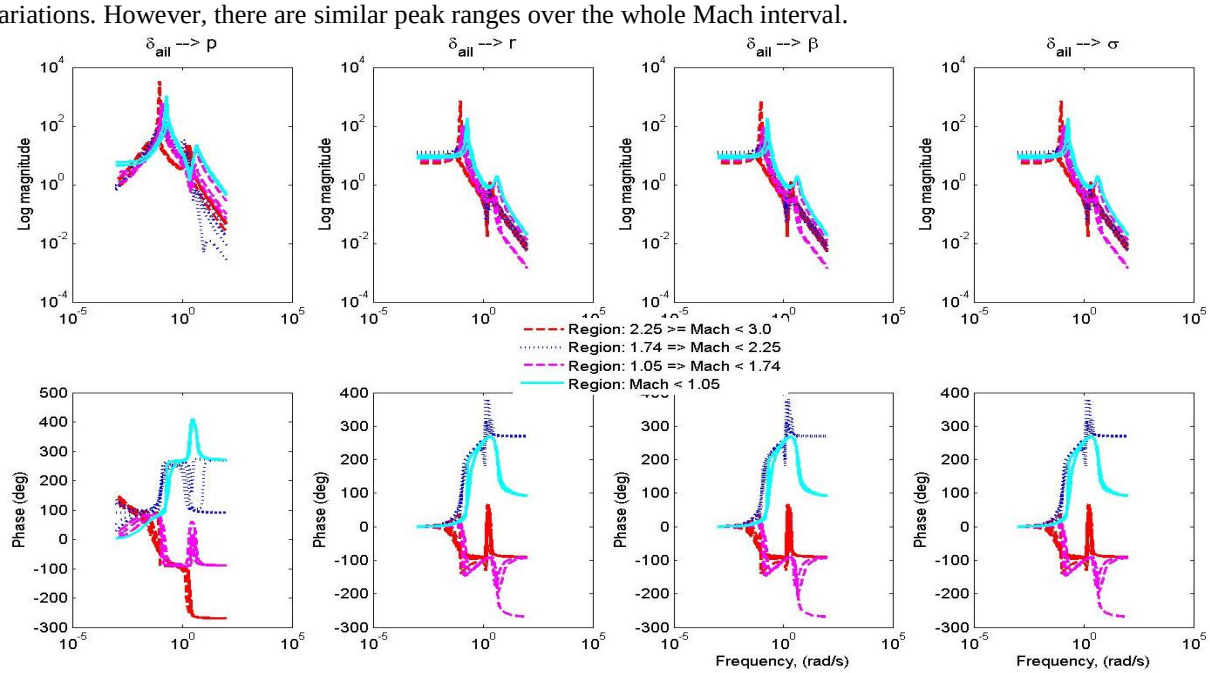

Figure II-8 Dynamic variations in the lateral/directional motion: Bode plots based on Mach regions

III. Baseline H_∞ and LPV control design

Gain-scheduling is a well known and ad-hoc industrial methodology to design controllers for dynamical systems over a wide performance envelope [4, 5, 6]. Usually, a family of local LTI controllers that are designed based on local LTI plants are linearly interpolated, yielding a controller that globally stabilizes the system and satisfies the required performance specifications sufficiently well. If, however, parametric uncertainties significantly change the behavior of the local LTI models, it is also required to robustify the local LTI controllers with respect to these parametric uncertainties. This can complicate the design of a gain-scheduled controller drastically. Although it is not impossible to design a gain-scheduling controller that is robust against large parameter variations, this is usually only possible by performing numerous ad-hoc synthesis-analysis iterations. Moreover, the local LTI controllers only guarantee stability and performance for the local linearized plant. Therefore, the gain-scheduled methodology is considered ad-hoc, resulting in cumbersome iterative design procedures.

During the last two decades, LPV control has been presented as a very promising technique to overcome these problems in a reliable and systematic fashion. LPV controller synthesis techniques naturally fit into the gain-scheduling framework, while imbuing it with stability and performance guarantees. Indeed, in LPV control, time-varying parameters (also called scheduling variables) that affect the plant are assumed to be measurable on-line. This essential data is taken into account by means of a scheduling function, which interacts with the controller in order to adapt to the constantly changing environmental conditions. A great amount of algorithms for the automated synthesis of LPV controllers have been proposed in the literature, each with its own importance and features. Various methods (i.e. polytopic, LFT or non-LFT, for infinite or bounded parameter rates, with or without parameter space gridding, convex or non convex) are now readily available [1, 2, 3, 12, 13, 14, 21, 45, 22].

This section summarizes the development of two controllers for the high-fidelity re-entry benchmark problem. The first controller (called baseline) is an H_∞ gain-scheduling controller [31] and the (advanced) controller is based on the LPV synthesis approach called Single Quadratic Lyapunov Function (SQLF). The control objectives for both designs are to track the reference angles of-attack, sideslip and bank in the presence of the established noise as well as the parametric uncertainties with desired deviations of less than 2 degrees and acceptable short-time deviations of less than 4 degrees.

A. Baseline gain-scheduling H_∞ controller design

H_∞ controller synthesis is a design technique where the specification of performance and robustness objectives is the main driver in correctly posing a mathematical optimization problem, as opposed to classical control synthesis techniques where the satisfaction of these objectives is evaluated after the design. Indeed, H_∞ controller synthesis techniques have become the cornerstone for modern control and are widely applied throughout industry [2, 6, 8].

Due to the characteristics of the system (see Section II-B) it is not possible to design a single H_∞ controller that provides acceptable global performance for the full motion and Mach region. Therefore, ad-hoc gain-scheduling control design is performed based on local LTI models and H_∞ theory. Similarly, a decoupled design approach is followed to parallel the most standard control design process used for this type of vehicles in industry.

The main steps for gain-scheduled H_∞ synthesis are:

- <u>Design local H_∞ controllers along the flight envelope.</u> Although it is decided to apply the H_∞ controller synthesis technique these local-designs can be obtained by any control design method. The two key steps, besides the H_∞ controller synthesis itself, are (i) the selection of the trim points along the flight envelope at which it is desired to perform the controller designs, and (ii) defining the gain-scheduled framework (e.g. state-space matrices or controller output interpolation). Although the latter issue is more appropriately considered within the next step, it is introduced here as its definition has a critical influence on the local controller designs. For example, output interpolation requires that the controllers share a common output structure while state-space matrix interpolation requires that they share the same input/output/state structure.

- <u>Gain-scheduling or interpolation of the (local) H_∞ controllers</u>. In the classical gain-scheduling process this step is ad-hoc and consumes most of the designer's time without providing guarantees on the performance and robustness properties of the global design. Key issues on this step are (i) the selection of the scheduling parameters and (ii) the selection of the interpolation rule.

Controller design for the longitudinal motion

The design rationale for the industrial benchmark longitudinal motion is that of angle-of-attack tracking through an ideal-model formulation. Since only the inner-loop control is considered, it is possible to consider the short-period motion only. In this fashion, the state dimension of the H_∞ controllers is also reduced since the H_∞ synthesis technique yield controllers with the same number of states as the weighted (generalized) plant.

The open-loop LTI plants used for the synthesis of the H_∞ controllers have 2 states (the angle-of-attack and pitch rate), two outputs (identical to the states) and two inputs (the elevator and speed-brake deflections). The weighted open-loop interconnection used for the H_∞ synthesis is given in Figure III-1 for the longitudinal motion. *Wact* is a low-pass filter that penalizes the actuators magnitude; *Wrob* is used to add uncertainty at the plant input; *Wperf* and *Wid* serve to model the angle-of-attack tracking formulation and to penalize its error; *Wcmd* shapes the angle-of-attack input; and finally, *Wnoise* is used for robustness by shaping the noise effect on the system. The *act*-block represents the model of the actuators and is chosen to be and identity (*I*) for the longitudinal motion.

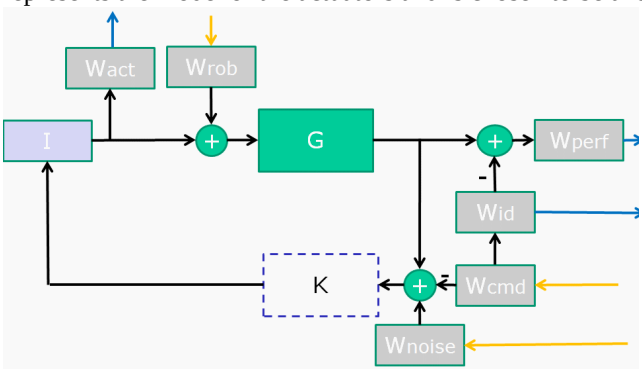

Figure III-1 Enhanced HL20 longitudinal baseline K: H_∞design interconnection

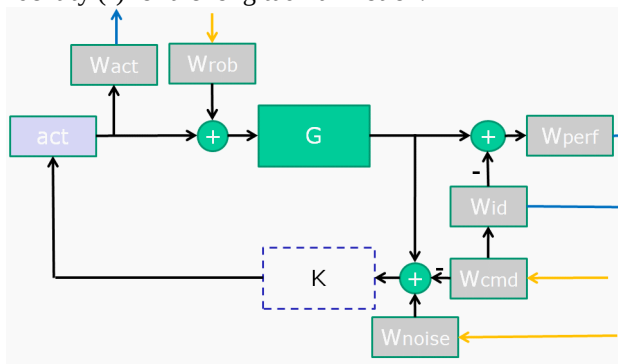

Figure III-2 Enhanced HL20 Lat/Dir baseline K: H_∞design interconnection

Assuming no interaction with the lateral/directional controller, it is possible to design a single H_∞ longitudinal controller that performs sufficiently well for the entire Mach interval. However, when the full motion is considered the interaction between the longitudinal and lateral/directional aerodynamic surfaces (arising from the control-mixer) leads to an unacceptable loss of performance. Thus, a gain-scheduled approach is followed also for the longitudinal motion in order to ameliorate the effect of the coupled aerodynamic surfaces while satisfying the requirement to stay as close as possible to the standard (decoupled) control design process for space applications.

A controller output interpolation scheme is selected. This has the advantage of avoiding numerical issues with the state-space matrix interpolation as well as issues such as state convergence, dwelling time, initial condition and CPU load processing. The key problem in controller output interpolation, on the other hand, is to ensure that wind-up does not occur. This can be accomplished by enforcing the deflection magnitudes to be of similar size and sign (i.e. avoiding one controller demanding +20deg deflection and the other -20deg for the same surface). It is chosen to linearly interpolate the local H_∞ controllers based on Mach number since this parameter is a relatively standard measurable signal that can be effectively used to detect the system dynamic changes along the re-entry trajectory.

The selection of the Mach number set that defines the interpolation intervals is by no means trivial and can be very cumbersome. The trim points are selected by starting at the upper extreme in the re-entry trajectory, synthesizing a local H_∞ controller at that point, and subsequently analyzing its linear performance and robustness properties by means of frequency and time domain analysis along the re-entry trajectory until performance is lost. Once this occurs, a re-design is attempted to enlarge the covered domain. This can be repeated until we are satisfied with the performance of the local controller. The selected trim for the longitudinal motion covering the Mach region of interest are at M=3.95 (corresponding to flight time at 1650 seconds) and M=0.92 (time=1850 seconds).

Controller design for the lateral/directional motion

The (local) lateral/directional open-loop LTI plants used for the design consist of four states (yaw rate r, roll rate p, sideslip angle β and bank angle ϕ), two input channels (aileron δ_{ail} and rudder δ_{rud} deflections) and four outputs (yaw rate, roll rate, lateral acceleration n_y and bank angle). As mentioned above, all attempts to design a single LTI controller for this motion are futile. Moreover, due to the control mix logic, which directly couples the aileron and

elevon demands, the design of the de-coupled lateral/directional and longitudinal controllers becomes quite iterative and ad-hoc.

Figure III-2 above shows the design interconnection used for the synthesis of the local lateral/directional H_∞ controllers. A model-matching approach for bank angle commands (W_{cmd} and W_{id}) is considered. Furthermore, the lateral acceleration minimization and turn-coordination are two additional objectives included in the performance weight W_{perf}. The latter performance objective is represented as $TC=r-0.037\phi$, following [7]. The key difference between the longitudinal and lateral/directional design is a first-order model for the actuators *act* which are used in addition to actuator weights W_{act}. This not only limits the magnitude but also, more importantly, the actuators rate. The robustness weight W_{rob}, again, is used to add uncertainty to the input of the plant in order to handle the challenging parametric and aerodynamic uncertainties. Following the approach for the longitudinal motion, the gain scheduling design process starts by selecting the highest Mach number in the considered trajectory and establishing its coverage region before proceeding with the subsequent local controller design. Due to the higher complexity of the lateral/directional dynamics a larger number of local LTI H_∞ controllers and, hence, a larger number of controller interpolations are needed (see Figure III-3).

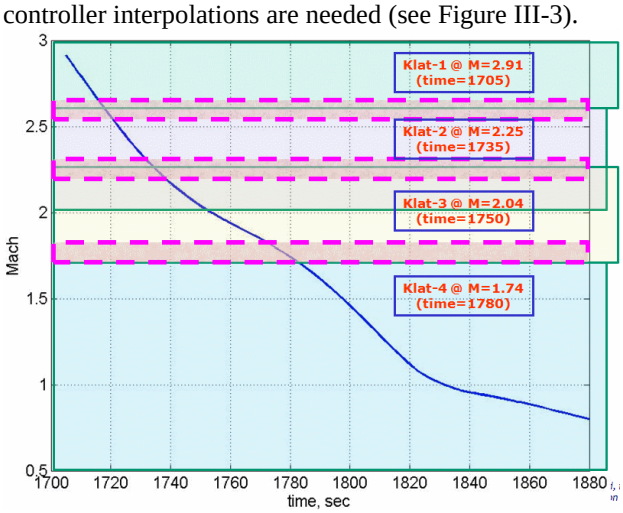

Figure III-3 Lateral/directional baseline gain-scheduled controller interpolation scheme

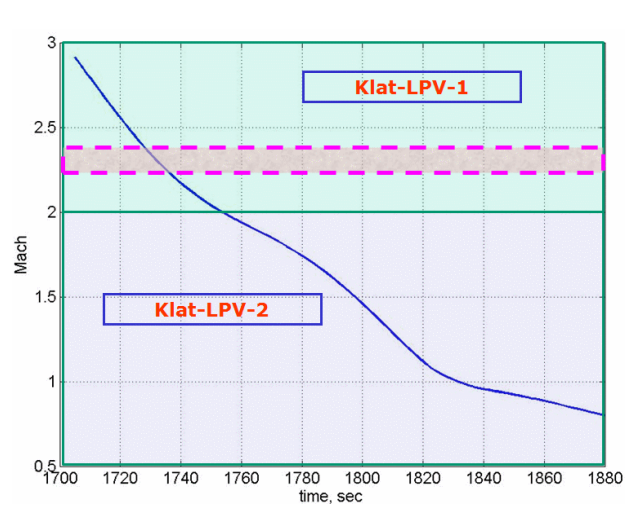

Figure III-4 Lateral/directional LPV controller interpolation scheme

B. LPV controller design based on the Single Quadratic Lyapunov Function (SQLF) approach

An alternative approach to standard gain-scheduling is to use LPV/LFT synthesis techniques such as the single quadratic Lyapunov function (SQLF) approach, which is based on H_∞ theory:

Theorem 1 SQLF Bounded Real Lemma [32] *Given the LPV system $(A(\rho), B(\rho), C(\rho), D(\rho))$ and a scalar $\gamma>0$. If there exists a $P\in\Re^{nxn}$, $P=P^T>0$ such that for all ρ*

$$\begin{bmatrix} A(\rho)^T P + PA(\rho) & PB(\rho) & C(\rho)^T \\ B(\rho)^T P & -\gamma^2 I & D(\rho)^T \\ C(\rho) & D(\rho) & -I \end{bmatrix} < 0, \qquad (8)$$

then the LPV system is quadratically stable and the L_2-gain of the LPV systems is smaller than γ.

In essence, the resulting synthesis technique relies on guaranteeing closed-loop stability and performance by a single quadratic Lyapunov function that is independent of the scheduling vector (i.e. $V(x) = x^TPx$ where x represents the state). The main advantage of the employed design algorithm is that it directly builds on the H_∞-design framework. Indeed, the software implementation of the employed technique directly takes (with minor modifications) the design weights and interconnection used for the synthesis of the local H_∞ controllers in order to synthesize the LPV controller.

It is remarked at this point that the tuning of the weights can be performed much faster for the LPV synthesis than for the baseline approach due to the global automated scheduling of the approach. In order to obtain a similar level of performance and robustness with the baseline controllers, as achieved with the LPV controller, a much more

time-consuming weight tuning process is required. Moreover, it is worth mentioning that the direct use of the final LPV weights and local (linearized) LTI plants for the ad-hoc gain-scheduling does not result in similar performance and robustness properties. In summary, the systematic character of the LPV synthesis techniques can save a lot of time in defining the weights and in achieving the required control design objectives if compared to ad-hoc gain-scheduling.

Controller design for the longitudinal and lateral/directional motions

The design objectives and interconnection used for the synthesis of the longitudinal baseline gain-scheduled H_∞ controller are also used for the synthesis of the longitudinal LPV controller. The only modifications that are made are the use of a more refined grid of local (linearized) LTI plants and a slight modification of the weights. Despite an apparent increase in design complexity, four different sets of weights are required for the LPV controller as opposed to three for the baseline controller, the resulting LPV controller is a single dynamic system and no effort on ad-hoc manual gain-scheduling is required (which after all is one of the greatest advantages of LPV synthesis techniques).

As is the case for the lateral/directional gain-scheduled baseline H_∞ controller, the lateral/directional LPV controller is much more complex if compared to the controllers for the longitudinal motion. Therefore, it is necessary to design two LPV controllers and linearly interpolate them in the same fashion as done for the baseline gain-scheduling controllers. Nevertheless, the use of LPV synthesis techniques reduces the complexity of the design process significantly. As can be seen in Figure III-3 and Figure III-4 only one interpolation is needed for the LPV controller versus three for the gain-scheduled H_∞ controller.

C. Monte Carlo campaign results

The design process of the controllers concludes with a summary of the Monte Carlo (MC) campaigns. The analysis is performed for both the baseline H_∞ controller as well as the LPV controller using the full nonlinear motion simulator. The MC campaign is performed using 1000 random runs, covering the full 100 percent of the uncertainty ranges given in Table II-3. In addition 400 additional random runs are performed, half covering only 80 of the uncertainty range and the other half 90 percent. This allows to assess the robustness levels of the controllers for different uncertainty ranges. The results are shown in Table III-1.

Table III-1 Percentage of failed cases in the Monte Carlo simulations

Controller	Uncertainty range: % of Δ_{max} [number of runs]		
	80 % [200]	90 % [200]	100 % [1000]
GS H-infinity	2 %	5 %	7.1 %
SQLF-LPV	0 %	0 %	0 %

As can be seen, the LPV-SQLF controller passed all runs successfully while the baseline H_∞ controller failed in 2, 5 and 7 percent of the runs for the 80, 90 and 100 percent of the uncertainty ranges respectively. Hence, whereas the LPV controller completely satisfied all the robustness objectives, the baseline H_∞ controller failed in these objectives in more than 7 percent of the simulations. It is also worth mentioning that a min/nom/max uncertainty nonlinear simulation did not reveal this shortcoming on the robustness of the baseline H_∞ controller.

Figure III-5 and Figure III-6 show the outputs of the (full 6 degrees-of-freedom) Monte Carlo campaigns performed for each controller. Note that in comparison to the LPV controller, the baseline H_∞ controller shows a significant degradation of performance on the time intervals [1715-1735] and [1756-1780]. These intervals coincide with the controller interpolation regions shown in Figure III-3 and the change of the angle-of-attack into a constant steady-state value respectively. This nicely illustrates the advantages of the LPV synthesis techniques.

A detailed investigation, by means of time consuming signal examination and additional dedicated time-domain simulations, showed that this degradation is caused by the ad-hoc interpolation that is performed for the baseline H_∞ controller. This resulted in significant actuator saturations, leading to performance degradation, and, in some cases, even to stability loss (as can be seen in Table III-1). As already mentioned, improvement of the baseline H_∞ controller would require much more time-consuming fine tuning of the individual (local) H_∞ controllers and the controller interpolation schemes. It is highlighted at this point that these types of problems (i.e. the effect of interpolation, saturation and motion coupling) cannot be analyzed with standard linear techniques. The designer, hence, might face the need for an expensive retuning or redesign only after a time consuming and expensive Monte Carlo campaign is performed. In Section V it is shown how LPV/LFT analysis techniques such as IQC analysis are used to identify these issues in a quick, clear and reliable fashion.

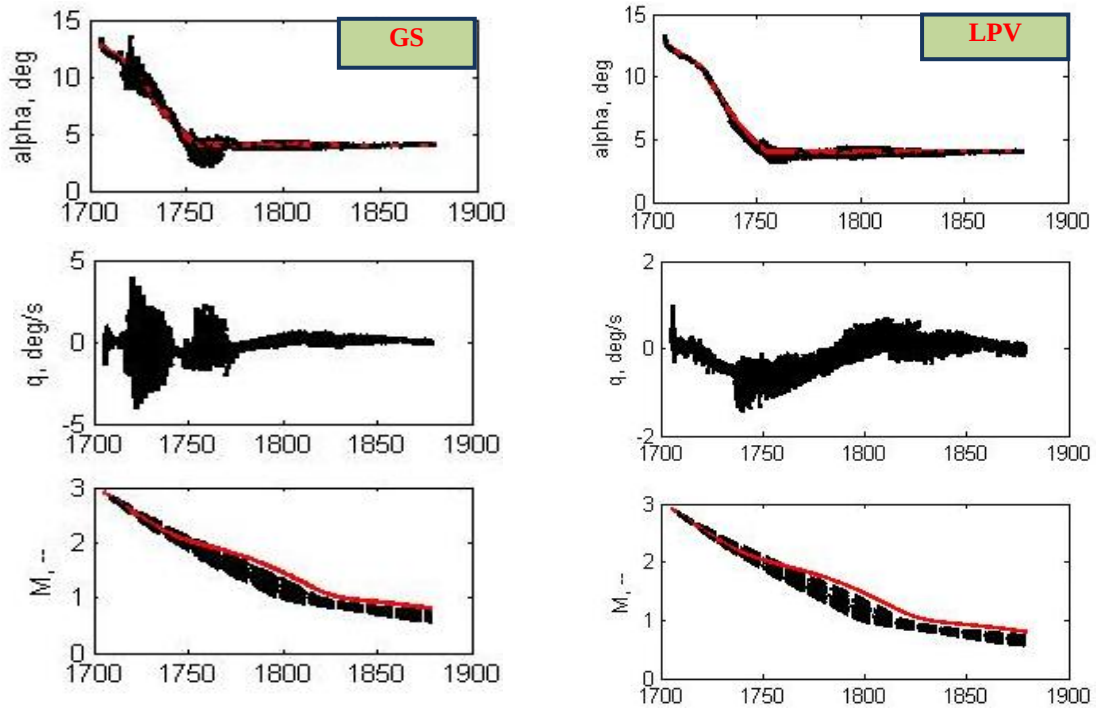

Figure III-5 Monte Carlo analysis (plotted: 100 out of 1000 runs): longitudinal outputs GS vs LPV

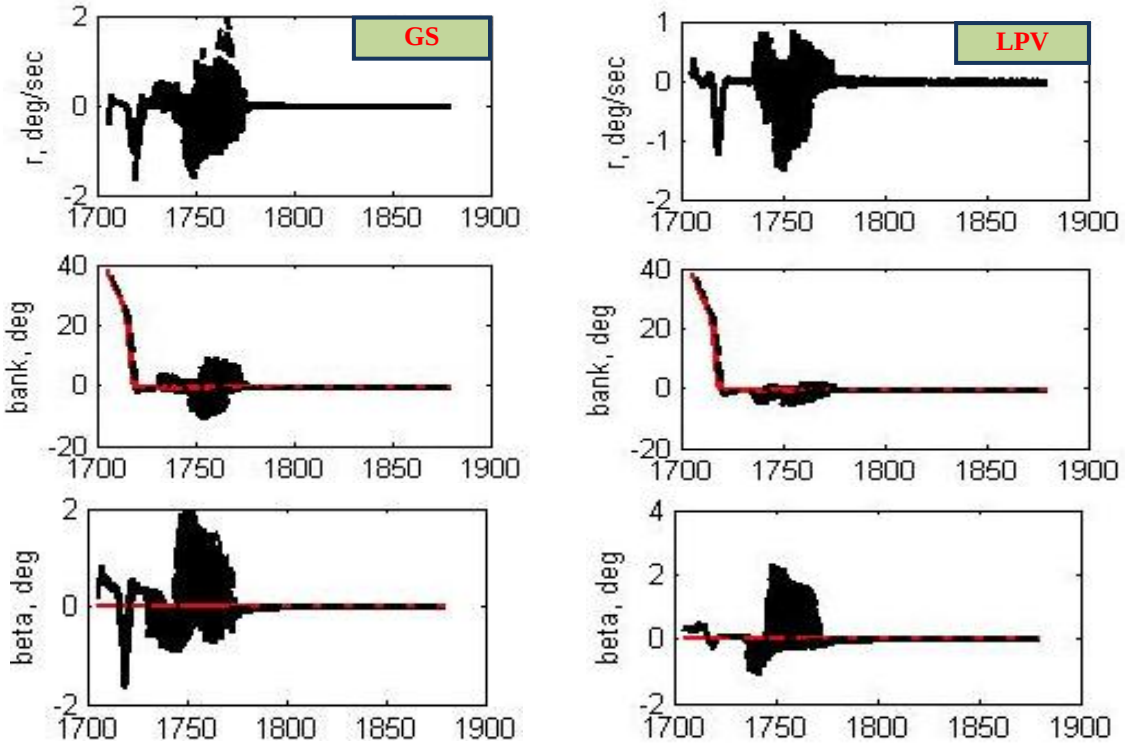

Figure III-6 Monte Carlo analysis (plotted: 100 out of 1000 runs): lat/dir outputs GS vs LPV

IV. LFT/LPV modeling for analysis

A powerful model representation used in modern control is the linear fractional transformation (LFT) [1, 20]. An LFT is a feedback interconnection of a nominal LTI plant M and a block-diagonally structured, bounded and causal operator Δ (see Figure IV-1). Powerful analysis techniques arising from modern control are often based on LPV concepts and models that rely on representing a system in the LFT form. Indeed, LPV systems, and in full generality nonlinear systems given by polynomial or rational expressions, can be represented as LFT models where the time-varying parameters and the uncertain or nonlinear terms are collected in the Δ-block and the (nominal) LTI part in M. Obtaining an LPV/LFT model from a general nonlinear system, however, is by no means straightforward [9, 10, 15, 20, 21]. One of the main challenges is to keep the dimensions of the Δ block small (in terms of parameters and their number repetitions).

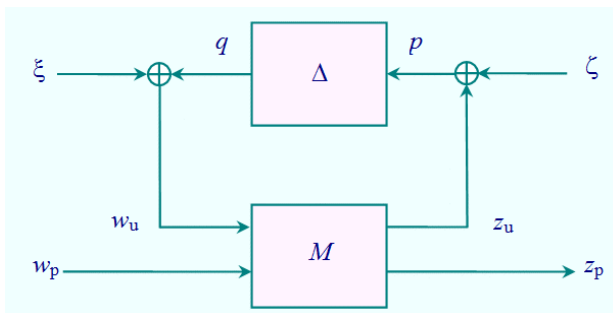

Figure IV-1 LFT representations: setup for robust stability and performance analysis

The main idea behind using LPV in lieu of LTI representations is to account for time-varying dynamics by exploiting the use of online measurable scheduling variables. This enables us to design and analyze time-varying dynamical systems. Moreover, in comparison to Linear Time-Varying (LTV) systems, LPV approaches do not require anti-causal knowledge on the time varying vector (i.e. LTV systems often assume future and past knowledge) since all what they require is the scheduling parameter to be measurable and to belong to a closed set.

LFT models of the benchmark problem can be obtained by favor of the LPVMAD modeling toolbox [15] using a Simulink-based uncertain LTI-LFT modeling algorithm followed by a symbolic interpolation-based LPV-LFT modeling algorithm. The toolbox yields LPV-LFT models that depend on parametric uncertainties and scheduling variables. The fidelity of the LPV-LFT models can be influenced by changing the order of the polynomial interpolation or by narrowing down the interpolation interval. Increasing the fidelity of the models, however, comes at the price of a more computationally demanding analysis. The key for a proper LPV/LFT analysis is, hence, to find a good balance between the fidelity of the model and the computational demand of the analysis.

As previously mentioned, Mach number is selected as the scheduling variable for the benchmark problem (i.e. $\Delta_S=\delta_M I_n$ where δ_M represents the normalized version of Mach and I_n, $n \in Z^+$ the number of repetitions of δ_M). The considered parametric uncertainties (shown in Table II-3) include the center-of-gravity coordinates, the aerodynamic coefficients, the moments-of-inertia and the mass. The parametric uncertainties are collected in the block-diagonal operator $\Delta_U = blkdiag(x_{cg} I_2, y_{cg} I_2, z_{cg} I_2, C_X I_1, C_Y I_1, C_Z I_1, C_{ll} I_1, C_m I_1, C_n I_1, I_{XX} I_5, I_{YY} I_2, I_{ZZ} I_5, m I_6)$.

Evidently, it is crucial to validate the quality of the obtained LPV models. This can be done by fixing the scheduling variable as well as the parametric uncertainties at a grid of trim points and comparing, using established linear analyses, with the plants obtained through direct linearization of the nonlinear system at the same trim points. Figure IV-2, for example, shows the comparison of the eigenvalues of the frozen LTI plants that are obtained from two different LPV-LFT models with the eigenvalues of the LTI models that are obtained by direct numerical trimming and linearization of the nonlinear system. Another way of validating the fidelity of the LPV models is to construct the weighted closed-loop generalized LPV models and compute their H_∞ norms for a frozen parameter-by-parameter grid, see Figure IV-3.

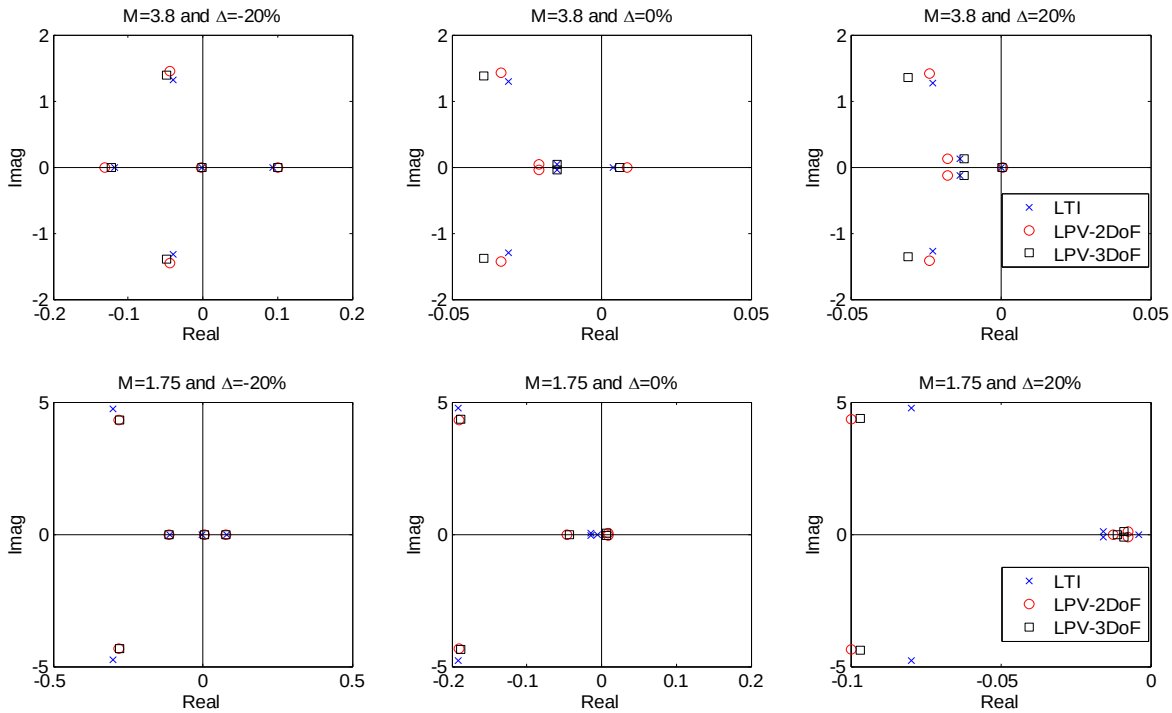

Figure IV-2 LPV model validation: eigenvalues LTI, LPV-2D & LPV-3D fit models

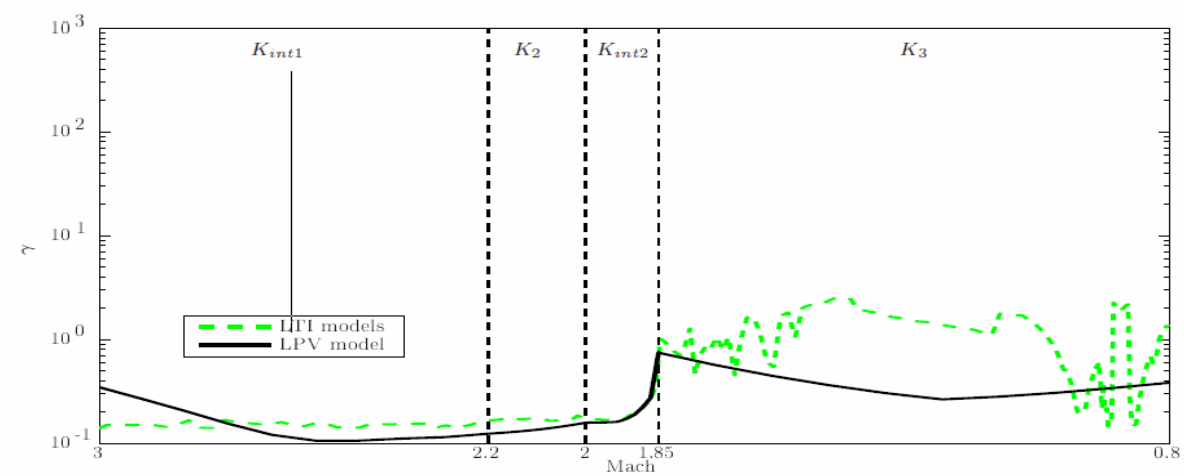

Figure IV-3 LPV model validation: weighted closed-loop H_∞ norm comparison

For the analysis of the longitudinal motion controllers, a single LPV model is generated based on a second order polynomial interpolation. Despite the fact that there is quite some mismatch between the H_∞ norms of the local closed-loop LTI models and the frozen parameter-by-parameter H_∞ norms of the global closed-loop LPV model in the region M∈[3-0.8], there is a good balance between the fidelity of the LPV model and the computational demand of the subsequent IQC analysis. Moreover, the analysis can be easily improved by, for example, generating two LPV models each defined on the intervals M∈ [3-1.85] and M∈ [1.85-0.8] respectively.

For the analysis of the lateral motion controllers, five LPV models are generated, all based on a second order polynomial interpolation. The complexity of the lateral motion is so high that it is not possible to verify frozen stability if only one LPV model is used for the whole Mach interval M∈ [3-0.8]. On the positive side, generating different models for smaller intervals improves the fidelity of the models while the complexity remains within feasible bounds. The analysis results using these LPV-LFT models and the designed controllers are summarized in the next section.

V. Analysis based on Integral Quadratic Constraints (IQC)

The main tools used for the analysis of controlled closed-loop systems rely on linear, analytical, frequency/time-domain techniques during the design phase and nonlinear computational-based time-domain techniques during the certification phase. In between these two "extremes" there is almost nothing that can guide the engineer in practical terms. Fortunately, there are many theoretical results addressing many of the problems found in this "analysis no-man's land". However, almost none of them are supported by reliable and efficient software tools. Moreover, these widely used analytical linear (e.g. gain/phase margins, rise/settling time) and computational nonlinear (i.e. Monte Carlo) techniques usually require different models, sometimes completely disconnected from the used controller synthesis techniques. This prevents the obtained information to be efficiently used in the re-design or returning of the controller.

LPV/LFT analysis techniques sit, from a theoretical and practical perspective, right in the middle of this analysis gap. This is largely due to their dependency on LPV/LFT models, which have a natural linear-nonlinear nature. Moreover, many developed analysis techniques for a great variety of uncertainty structures that were proposed for the LTI case can be readily extended to uncertain LPV systems taking into account certain non linear effects [11]. Similarly, the worst-case analysis techniques related to the Structured Singular Value (SSV) theory can be easily extended by employing the Integral Quadratic Constraint (IQC) framework. Also, worst-case perturbations can be generated by using dedicated lower bound SSV computations for LTI type of perturbations [12]. And finally, worst-case analysis with the inclusion of nonlinear effects can be specialized using the IQC approach together with results from the harmonic balance techniques. In summary, compared to traditional LTI/LTV analysis techniques, LPV analysis tools can:

- Guarantee stability against time-invariant and time-varying scheduling parameters using by (quadratic) Lyapunov function analysis (for the TV case only if the bounds on the parameter and its rate-of-variation are given).
- Capture and assess many relevant stability and performance tests in one unified framework, while offering the extra advantage of extensibility to dynamic and nonlinear and/or uncertainty components (through IQC analysis).
- Quantify the involved conservatism (at least for time-varying dynamic uncertainties and again, mostly by relying on IQC-based extensions).

In this section, a summary of the results of applying the IQC analysis techniques on the selected benchmark problem are presented and compared with the results from the nonlinear Monte Carlo campaign. It is important to highlight that the problems considered within the IQC framework cannot be addressed with other linear analytical techniques. Therefore, the capability and applicability validation of these advanced LPV/LFT analysis represent a step forward in closing the gap between linear design and nonlinear V&V.

A. IQC theoretical preliminaries

A cursory review of IQC theory is given first. Referring to the standard input-output setting for robust stability and performance analysis given in Figure IV-1, it is said that the system interconnection is (uniformly robustly L_2-) stable against the uncertainty set $\boldsymbol{U}$ if the induced L_2-norm $||(I-M\Delta)^{-1}||_{i2}$ is bounded on $\boldsymbol{U}$. If the system is robustly stable, finite-energy outputs (w_U, w_P, z_U and z_P) are obtained whenever $\Delta \in \boldsymbol{U}$ and the loop is excited by finite-energy inputs (ξ and ζ). In this case, the map from w_P to z_P is well-defined and given by the LFT $T_{Z_P W_P}=M_{PP}+M_{PU}(I-\Delta M_{UU})^{-1}M_{UP}$. Among various possible choices of performance indicators, consider again the induced L_2-gain of this map, $||T_{Z_P W_P}||_{i2}$. Then we say that M has robust L_2-gain performance of level γ if it is uniformly robustly stable against $\boldsymbol{U}$ and if $sup_{\Delta \in \boldsymbol{U}}||T_{Z_P W_P}||_{i2}<\gamma$.

Let us now describe the ingredients of the IQC analysis by first clarifying how the uncertainty can be described by an integral quadratic constraint. The finite-energy signals $q \in \mathbf{L}_2^{n_u}[0,\infty)$ and $p \in \mathbf{L}_2^{m_u}[0,\infty)$, whose Fourier transforms are denoted as ($\hat{q}, \hat{p}$), are said to satisfy the IQC defined by the IQC multiplier $\prod$ if:

$$\int_{-\infty}^{\infty}\begin{bmatrix}\hat{p}(j\omega)\\ \hat{q}(j\omega)\end{bmatrix}^{*}\underbrace{\begin{bmatrix}\Pi_{11}(j\omega) & \Pi_{12}(j\omega)\\ \Pi_{12}^{*}(j\omega) & \Pi_{22}(j\omega)\end{bmatrix}}_{\Pi(j\omega)}\begin{bmatrix}\hat{p}(j\omega)\\ \hat{q}(j\omega)\end{bmatrix}d\omega \geq 0 \cdot \tag{9}$$

The uncertainty that is introduced by an operator Δ is said to be described by an IQC of this form, provided that it is satisfied by all finite-energy signals p and $q=\Delta(p)$ (where $\Delta(p)$ should be read as the output of Δ when excited by p). Here, $\Pi : j\mathbf{R} \to \mathbf{C}^{(m_u+n_u)\times(m_u+n_u)}$ can in principle be any measurable Hermitian-valued function, though it is usually chosen among the rational functions that are bounded on the imaginary axis. For a given type of uncertainty, it is then possible to represent the set of suitable multipliers as (where τ is introduced to satisfy some IQC technicalities):

$$\mathbf{M_U} := \left\{ \Pi : \int_{-\infty}^{\infty}\begin{bmatrix}\hat{p}(j\omega)\\ \tau\hat{q}(j\omega)\end{bmatrix}^{*}\Pi(j\omega)\begin{bmatrix}\hat{p}(j\omega)\\ \tau\hat{q}(j\omega)\end{bmatrix}d\omega \geq 0, \forall\tau\in[0,1], \forall p\in\mathbf{L}_2^{m_u}, q=\Delta(p), \Delta\in\mathbf{U}\right\}, \tag{10}$$

With the multipliers chosen from the above set, analyzing whether the system is robustly stable and has robust performance of level $\gamma = \sqrt{\kappa}$ amounts, roughly speaking, to checking whether the following inequality is satisfied:

$$\begin{bmatrix}M(j\omega)\\ I\end{bmatrix}^{*}\tilde{\Pi}(j\omega)\begin{bmatrix}M(j\omega)\\ I\end{bmatrix} \prec 0,\ \forall\omega\in\mathbf{R}\cup\{\infty\}, \text{ where } \tilde{\Pi} = \begin{bmatrix}\Pi_{11} & 0 & \Pi_{12} & 0\\ 0 & I & 0 & 0\\ \Pi_{12}^{*} & 0 & \Pi_{22} & 0\\ 0 & 0 & 0 & -\kappa I\end{bmatrix}. \tag{11}$$

B. IQC analysis of the baseline and LPV controllers

For the controllers in Section III, IQC analyses are performed to demonstrate the robust stability and performance characteristics of the designs with respect to the following issues:

- The applied interpolation schemes
- LTV perturbations
- Parametric uncertainties
- Actuator saturation nonlinearities
- Time delays

In this section a summary of the results is presented, i.e. for the interpolation and LTV issues.

Controller interpolation analysis

As mentioned above and observed in Section III-C, there is a noticeable drop in robust performance for the implemented baseline in comparison to the LPV controller. It is not possible to analyze this performance drop using standard linear analysis techniques, since it is (revealed by dedicated and time-consuming analysis) caused by a combination of time-varying behavior, motion coupling and saturation.

Figure V-1 shows a summary of the controller interpolation IQC analysis and including in the bottom row the nonlinear, time-domain responses for angle-of-attack tracking. Two important conclusions can be made based on this figure:

- It is very nicely illustrated that interpolation of controllers causes the performance to degrade significantly and that this problem can be much better handled or even overcomed by employing the LPV controller synthesis methodology.
- The figure shows that the IQC analysis tools can be adopted very efficiently in order to analytically analyze the performance of the closed-loop system before resorting to (much) more time consuming simulation analysis methods such as Monte Carlo.

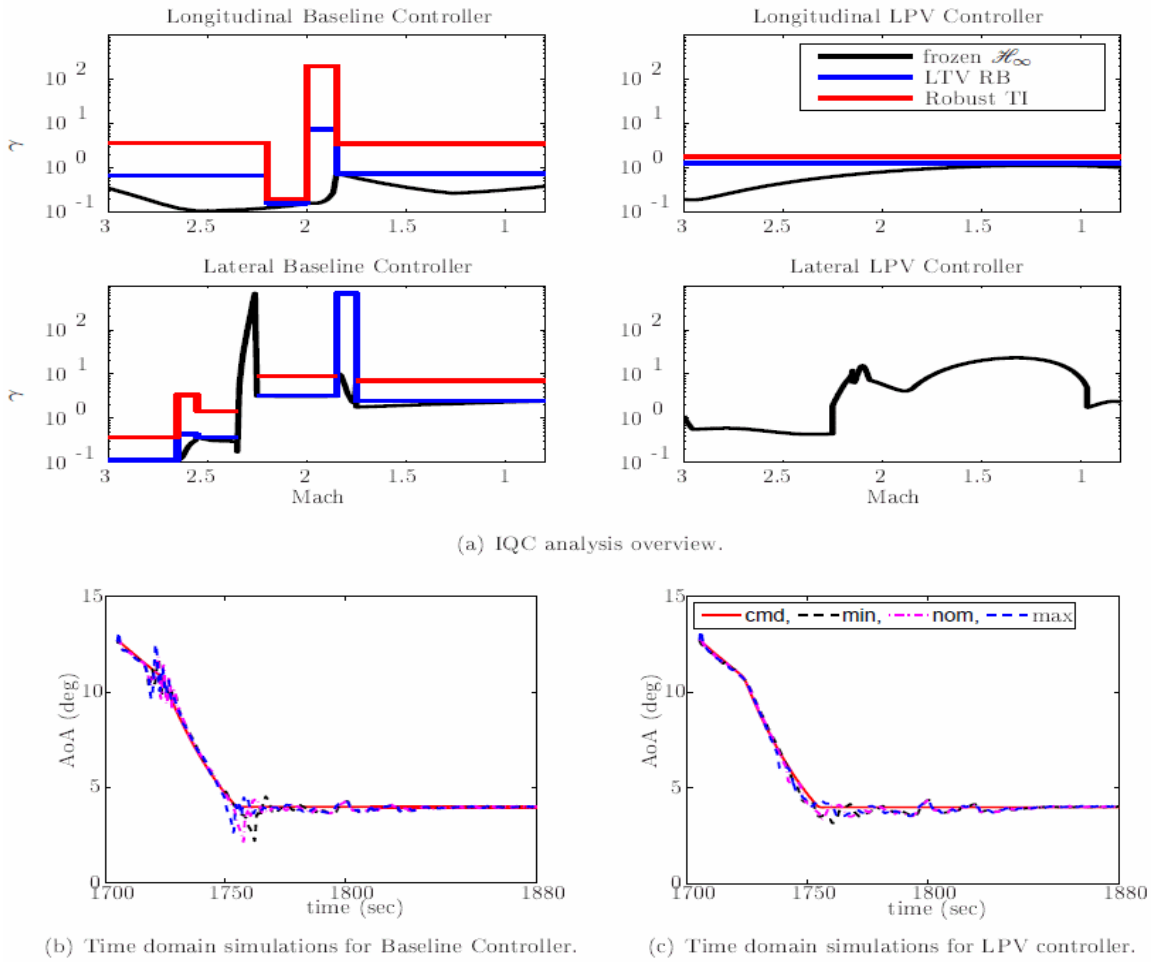

Figure V-1 Controller interpolation analysis for: baseline (left) and LPV (right) full-motion controllers using IQC analysis (a) and nonlinear simulation analysis (b & c).

Linear-Time-Varying parametric uncertainty analysis

The Robust control toolbox [20, 23] does not have an analysis tool that can be applied to LPV systems with general rational dependence on structured time-varying parametric uncertainties. It is possible to employ either conservative analysis tools like those based on the small-gain theorem, or resort to the heuristic approach of using μ analysis for the purposes of investigating robust stability and performance against slowly time-varying parametric uncertainties, if considering general rational parameter dependence. One of the prominent features of the IQC analysis tool [16], on the other hand, is that it facilitates a rigorous analysis of robust stability and performance against smooth parameter variations. It is even possible to take into account the correlation between the parameters and their rates-of-variation.

In Figure V-2 the results of the IQC analysis are shown for time-varying Mach in the longitudinal baseline (top) and LPV (bottom) controllers. The analysis is performed on the nominal weighted closed-loop system interconnection (i.e. $\Delta_U=0$) for the case where Mach is allowed to vary arbitrarily fast (IQC LTV AF) as well as for the case where it is rate-bounded (IQC LTV RB). As can be seen the L_2-gain performance of the baseline controller degrades drastically in the interpolation regions if Mach is allowed to vary arbitrarily fast. Fortunately, if the rate-of-variation is taken into account the IQC analysis results improve significantly. For some regions even the time-invariant case is (almost) recovered, which implies exactness. For the LPV controller (bottom plot) the IQC analysis confirms the drastic improvements seen in the nonlinear simulations.

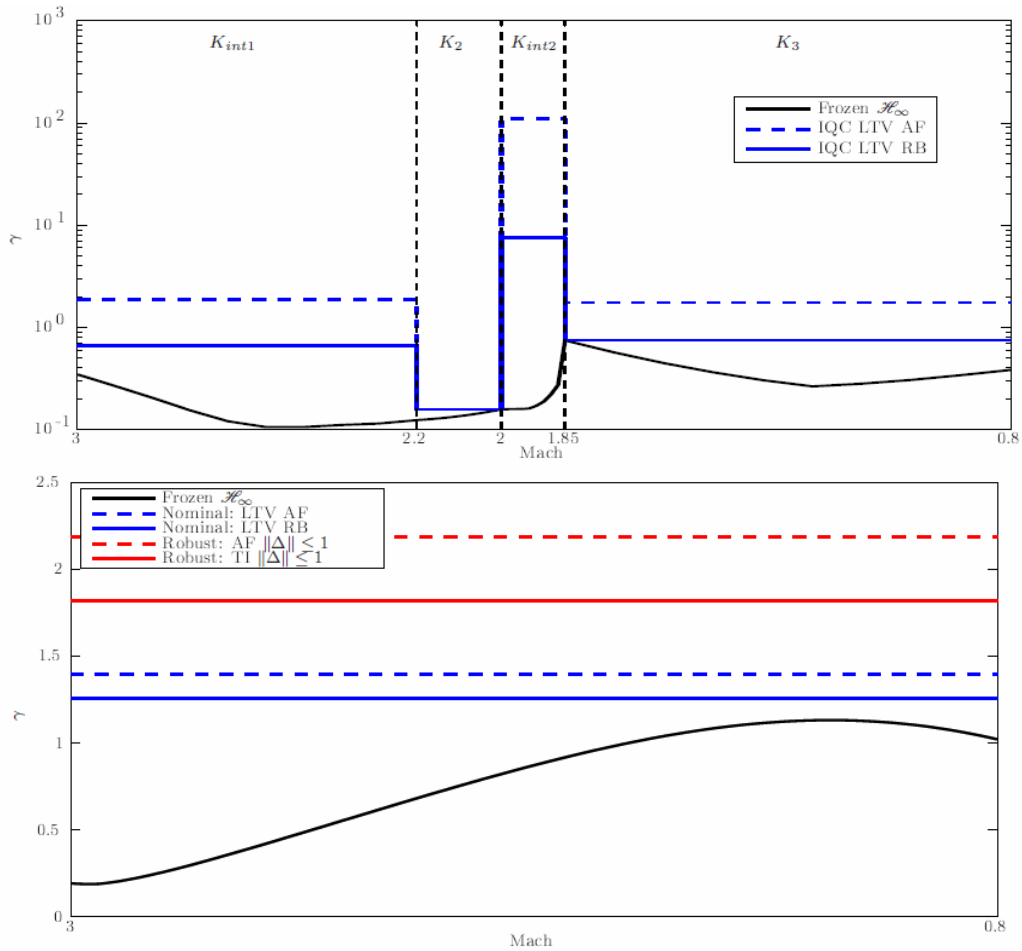

Figure V-2 LPVMAD IQC LTV analysis for: baseline (top) and LPV (bottom) controllers

VI. Conclusion

In this paper the advantages and capabilities of LPV design, modeling and analysis techniques for their use in a control design process of a space application have been presented. A high-fidelity version of an atmospheric re-entry vehicle has been developed in order to apply and demonstrate the techniques. For comparison reasons the design of a (baseline) gain-scheduling H_∞ controller has been also considered. The results indicate that: (i) LPV controller synthesis techniques can help to overcome some of the stringent drawbacks in gain-scheduling controller design, (ii) IQC analysis methods can be used very efficiently to accurately interpret the nonlinear time domain simulation results (which allow to close the gap between linear design and nonlinear V&V while directly providing information for redesign and/or retuning through the quantification of performance degradation), and, (iii) the key support of LFT/LPV modeling for analysis of realistic and challenging problems (including the incorporation of the controller interpolation scheme, parametric uncertainty and even nonlinearities within the LFT framework).

Acknowledgments

The authors would like to thank Dr. Luis F. Peñín, head of the GNC/AOCSS division at Deimos Space as well as the rest of the LPVMAD principal investigators and their teams: Dr. Declan Bates (University of Leicester) and professor József Bokor (Hungarian Academia of Sciences Automatic Control Lab, SZTAKI) for their help and comments, and to Dr. Mazen Farhood for his contributions to the development of the IQC toolboxes. Finally, professor Gary Balas from the University of Minnesota is gratefully acknowledge for providing the LPV SQLF software tools used for the LPV controller design. The LPVMAD project is funded by the European Space Agency under ESA-ESTEC contract 20565/07/NL/GLC.

References

[1] Packard, A., "Gain-scheduling via Linear Fractional Transformations," *Systems and Control Letters*, 22, 79-92, 1994

[2] P. Gahinet, P. Apkarian, "A linear matrix inequality approach to H-infinity control," *International Journal of Robust and Nonlinear Control*, 4:421–448, 1994

[3] Wu, F., "Control of Liner Parameter Varying Systems," Ph.D. Dissertation, Dept. of Engineering, Univ. of California, Berkeley, 1995

[4] Rugh, W.J., Shamma, F., "Research on Gain Scheduling," *Automatica*, Vol. 36, 2000, pp. 1401–1425

[5] Leith, D.J., Leithead, W.E., "Survey of Gain-Scheduling Analysis and Design," *International Journal of Control*, Vol. 73, No. 11, 2000, pp. 1001–1025

[6] Balas, G.J., "Flight control law design: An industry perspective", *European Control Conference*, September 2003

[7] Doyle, J.C, Lenz, K., Packard, A., "Design examples using mu-synthesis: Space shuttle lateral axis FCS during re-entry" *IEEE Control Decision Conference*, Vol. 25, pp 2218-2223, December 1986

[8] Fujimori, A., Terui, F., Nikiforuk, P. "Flight Control Design of an Unmanned Space Vehicle Using Gain Scheduling" *AIAA Journal of Guidance, Control and Dynamics*, Vol.28, No.1, 2005.

[9] Marcos A., Balas, G.J., "Development of Linear Parameter Varying Models for Aircraft," *AIAA Journal of Guidance, Control, and Dynamics* Vol. 27, No. 2, March April 2004

[10] Weehong Tan, Packard, A.K., Balas, G.J., "Quasi-LPV modeling and LPV control of a generic missile," *American Control Conference*, Vol. 5, pp. 3692-3696, 2000

[11] Papageorgiou, C., K. Glover, "Robustness Analysis of Nonlinear Flight Controllers," *AIAA Journal of Guidance, Control and Dynamics*, Vol. 28, No 4, 2005

[12] Scherer, C.W., "Relaxations for Robust Linear Matrix Inequality Problems with Verifications for Exactness," *SIAM Journal on Matrix Analysis and Applications*, Vol. 27, No. 2, 2005

[13] Scherer, C.W., "LMI Relaxations in Robust Control," *European Journal of Control*, Vol. 12, No.1, 2006

[14] Lu, B., Wu, F., and Kim, S.W., "Switching LPV control of an F-16 aircraft via controller state reset", *IEEE Transactions on Control System Technology*, Vol. 14, Issue 2, March 2006

[15] Marcos, A., Kerr, M., De Zaiacomo, G., Peñín, L.F., Szabó, Z., Bokor, J., Rodony, G., "Application of LFT/LPV Modeling and Data-based Validation to a Re-entry Vehicle," *AIAA Guidance, Navigation and Control Conference* 2009

[16] Veenman, J., Köroğlu, H., Scherer, C.W., "Analysis of the Controlled NASA HL20 Atmospheric Re-entry Vehicle based on Dynamic IQCs," *AIAA Guidance, Navigation and Control Conference* 2009

[17] Veenman, J., Scherer, C.W., Köroğlu, H., "IQC-Based LPV Controller Synthesis for the NASA HL20 Atmospheric Re-entry Vehicle," *AIAA Guidance, Navigation and Control Conference* 2009

[18] Menon, P.P., Prempain, E., Postlethwaite, I., Bates, D., Bennani, S., "An LPV loop shaping controller design for the NASA HL-20 re-entry vehicle," *AIAA Guidance, Navigation and Control Conference* 2009

[19] Menon, P.P., Prempain, E., Postlethwaite, I., Bates, D., Bennani, S., "Nonlinear Worst-Case Analysis of an LPV Controller for Approach-Phase of a Re-entry Vehicle," *AIAA Guidance, Navigation and Control Conference* 2009

[20] Balas, G.J., Doyle, J.C., Glover, K., Packard, A., Smith, R. "μ-Analysis and Synthesis Toolbox", The Mathworks & Musyn Inc. June 1998

[21] Magni, J.F., "Linear Fractional Representation Toolbox: Modeling, order Reduction, Gain Scheduling", TR 6/08162 DCSD, ONERA, Systems Control and Flight Dynamics Department, Toulouse, France, January 2004

[22] Scherer C. W., S. Bennani, and E. Nijo, "Parametrically Varying Flight Control System Design with Full Block Scalings," *36th IEEE Conference on Decision and Control*, pages 1510–1515, San Diego, CA, 1997.

[23] Balas, G.J., Chiang, R., Packard, A., Safonov, M., "Robust Control Toolbox 3 User's Guide", The Mathworks. March 2007

[24] Marcos, A., Bennani, S., "LPV Modelling, Analysis and Design in Space Systems: Rationale, Objectives and Limitations," AIAA GNC Conference 2009

[25] Jackson, E.B., Cruz, C.I., Ragsdale, W.A. "Real-Time Simulation Model of the HL-20 Lifting Body", NASA Langley Technical Memorandum 107580, July 1992

[26] Jackson, E.B., Cruz, C.I. "Preliminary Subsonic Aerodynamic Model for Simulation Studies of the HL-20 Lifting Body" NASA Langley Technical Memorandum 4302, 1992

[27] Cruz, C.I., Ware, G.M. "Control Effectiveness and Tip-Fin Dihedral Effects for the HL-20 Lifting-Body Configuration at Mach Numbers from 1.6 to 4.5", NASA Langley Technical Memorandum 4697, 1995

[28] Scallion, W.I. "Aerodynamic Characteristics and Control Effectiveness of the HL-20 Lifting Body Configuration at Mach 10 in Air", NASA Langley Technical Memorandum 209357, September 1999

[29] Gage, S. "NASA HL-20 Lifting Body Airframe Modeled with Simulink and the Aerospace Blockset," Matlab Digest, Vol.10, No.4, July 2002, The Mathworks, http://www.mathworks.fr/company/newsletters/digest/july02/aero.html

[30] Powell, R.W. "Six-Degree-of-Freedom Guidance and Control-Entry Analysis of the HL-20" Journal of Spacecraft and Rockets, Vol.30, No.5, 1993

[31] Marcos, A., "A gain scheduled H-infinity controller for a re-entry benchmark," AIAA GNC Conference 2010

[32] Becker, G., "Quadratic stability and performance of linear parameter dependent systems," Ph.D. Dissertation, Dept. of Engineering, Univ. of California, Berkeley, 1993